Available online at www.sciencedirect.com
ScienceDirect
Optics Communications 277 (2007) 310–314
OPTICS COMMUNICATIONS
www.elsevier.com/locate/optcom

Methods of achieving linear index-change response for narrow-band fiber Bragg grating sequential writing

Kuei-Chu Hsu [a,*], Lih-Gen Sheu [b], Wei-Wei Hsiang [c], Yinchieh Lai [a]

[a] Department of Photonics and Institute of Electro-Optical Engineering, National Chiao-Tung University, Hsinchu 300, Taiwan, ROC
[b] Department of Electronic Engineering, Vanung University, Chung-Li, Tao-Yuan 320, Taiwan, ROC
[c] Department of Physics, Fu Jen Catholic University, Taipei 24205, Taiwan, ROC

Received 5 February 2007; received in revised form 30 April 2007; accepted 9 May 2007

Abstract

This investigation elucidates the refractive index-change response of the photosensitive optical fiber to exposed UV flux. The nonlinear UV photosensitivity deforms the index profile of FBGs on the tail edges where the writing UV flux is low. Pre-UV treatment eliminates the nonlinear index-change response and ensures the linearity of the response of subsequent grating writing. A new method that involves interference between two unequal beams in a single writing scan is proposed and demonstrated to be able to improve the index profile and the spectral response of fabricated FBGs. The procedure is stable for writing weak fiber Bragg gratings with pre-designed index profiles.

1. Introduction

Fiber Bragg grating (FBG) devices as narrowband filters and dispersion compensators have numerous applications in dense-wavelength-division-multiplexing (DWDM) systems and fiber lasers [1,2]. FBGs with complex grating index profiles and multiple phase-shifts can also be inversely designed to perform advanced filtering functions [3–5]. The relationship between the UV flux to which the device is exposed and the induced refractive index change must be calibrated carefully in fabricating precisely these complex grating profiles and phase-shifts. The induced index change in the fiber core is not a linear function of the exposed UV flux but a complicated curve [6]. The curve is nonlinear at low UV flux and linear elsewhere before saturation. For narrow-band FBG devices with long grating length and small index changes, the nonlinear photosensitivity makes difficult the realization of a perfect grating profile, influencing the reflection spectrum of the grating and degrading its performance. Accordingly, the UV writing must be conducted in the linear regime, so that an FBG with an arbitrary index modulation profile can be easily realized.

Pre-UV treatment is initially proposed to enhance the photosensitivity of optical fibers and increase the stability of the FBG devices [7], yet the advantage of the linear index response to pre-UV treatment in the matching of the target grating index profile has not been studied. In this work, the side-diffraction method is adopted to determine the refractive index profiles of fabricated FBGs more precisely. The linear grating index response is first examined using a single Gaussian UV shot with pre-UV treatment. This work demonstrates how pre-UV treatment helps to achieve a linear index change with UV flux, even though two writing scans are required. An improved method of unequal two-beam interference is then proposed to generate the required AC and DC amounts of UV flux in a single writing scan. This unequal interference setup provides greater stability in writing weak gratings in the linear regime.

* Corresponding author. Fax: +886 3 5716631.
E-mail addresses: jessica.eo91g@nctu.edu.tw, yclai@mail.nctu.edu.tw (K.-C. Hsu).

0030-4018/$ - see front matter © 2007 Elsevier B.V. All rights reserved.
doi:10.1016/j.optcom.2007.05.026

2. Nonlinear photosensitivity and pre-UV treatment

This work begins by calibrating more carefully than before the relationship between the induced change in the index of a photosensitive optical fiber and the UV flux to which it is exposed. The pre-UV treatment method is then performed to achieve a linear index-change response. Unlike in previous works [6,7], which assumed that the grating index profile was sinusoidal or uniform to fit the reflectivity, the side-diffraction method [8–12] is employed herein to scan the fiber grating and thus determine accurately the grating index modulation profile. An iterative procedure is then utilized to fit the reflection/transmission spectra, based on the transfer matrix method for determining the actual grating index modulation. The measured results reveal that the grating shape is deformed for simple writing schemes when the UV intensity is low. The relationship between the induced refractive index change and the exposed UV flux is nonlinear at low UV flux, such that the written grating index profile is deformed. As stated above, the pre-UV treatment can be performed in advance to prevent the nonlinear photosensitivity in the writing of a weak grating. The working principle of pre-UV treatment is to eliminate the nonlinear region using a DC bias flux so that the index change depends linearly on the UV flux, and the induced index profiles are similar to the envelope of the holographic writing UV beam.

The experiments are performed on fiber core (PS1500) photosensitive fibers, which were hydrogenated at a pressure of 1500 psi at room temperature for seven days. The UV source is a frequency-doubled CW argon-ion laser with an output wavelength of 244 nm. A Gaussian UV beam with a $1/e^2$ intensity beam radius of around 6.5 mm was used to imprint holographically the fiber Bragg grating in the fiber core. The induced refractive index profile was determined using the side-diffraction method. In the side-diffraction setup, the fiber is clamped on the translation stage with a sub-μm position monitoring resolution using an Agilent 5519A He–Ne laser interferometer, as shown in Fig. 1. A 35 mW high-power He–Ne laser beam with a diameter of 3 mm is divided into two beams: one is the probe beam and the other is the reference beam. The probe beam is focused onto the fiber grating under test with a spherical lens with a focal length of 20 cm. The first-order Bragg diffraction of the probe beam is generated under the phase-matching Bragg condition. This diffracted probe beam and the reference beam are combined at the beam combiner to form an interference pattern. A 440×480 monochrome CCD camera with a pixel width of 7.15 μm is utilized to record the interference pattern that is produced by the two beams. The CCD is proven to respond linearly to the He–Ne laser power and its S/N ratio is 50 dB. The refractive index profile is obtained by analyzing the visibility of the interference pattern along the entire grating. The polarization beam splitter enables the power ratio of the two beams to be controlled by adjusting the angles of the wave plates to yield good visibility contrast, even in the weak grating case. The variation in the refractive index is directly proportional to the visibility of the interference pattern of the two beams [12]. In the experimental setup herein, the minimum detectable refractive index variation of the grating is approximately 5×10^{-6}, depending on the probe laser power and the optimized intensity ratio of the divided two laser beams. Furthermore, an ASE light source and an optical spectrum analyzer are employed to measure the spectral response. The normalized refractive index profile is used directly to calculate the reflection and transmission spectra using the transfer matrix method. An iterative procedure is then applied to fit the measured spectra to determine the peak index modulation of the entire FBG.

Fig. 2a depicts the refractive index profiles that measured by the side-diffraction method for exposure to specified amounts of UV flux. The scan step of the translation stage is set to 100 μm. Fig. 2b plots the fitted peak refractive index modulation as a function of the UV flux at the center of grating. As expected, the change in the refractive index of the photosensitive fiber is nonlinear at low UV flux and linear thereafter (no saturation is observed at the UV flux of interest). The lowest UV flux case (15 J/cm^2) in Fig. 2a corresponds to the rapidly changing exponential-shaped relationship in Fig. 2b, which makes the grating index profile flat-topped. In previous works of mechanism studies [13], the photosensitization of optical fibers is modeled by a two-step process. The refractive index change is determined mainly by the concentration of Ge defect centers and defect sites for hydrogen reaction. The model indicates that the change in the refractive index curve at low

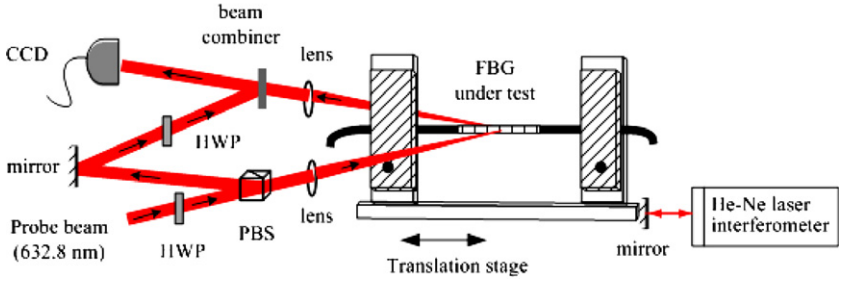

Fig. 1. Experimental setup of side-diffraction method. HWP: half wave plate, PBS: polarization beam splitter.

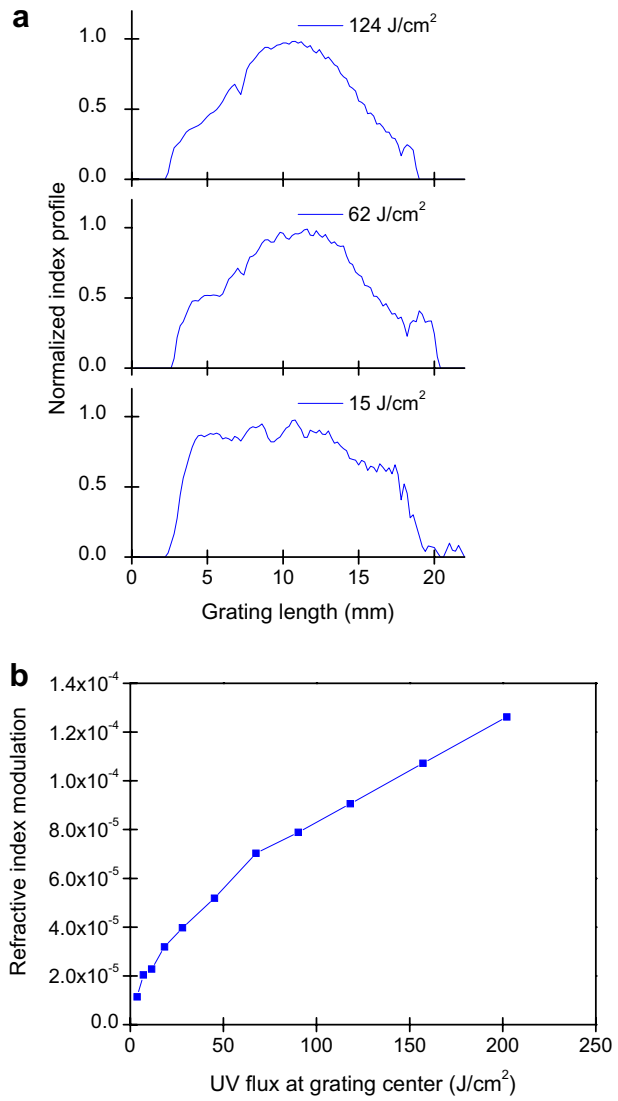

Fig. 2. (a) Refractive index modulation profile by a single Gaussian UV shot with a specific UV flux. (b) Refractive index modulation versus UV exposure flux.

UV flux has an exponential form, which result agrees with the measurements in Fig. 2b. Such nonlinear behavior causes the fiber grating index modulation profile to differ from the writing UV periodic intensity envelope. The shapes deform mostly at the tail edges of the Gaussian laser beam, where the UV intensity is low.

The pre-UV treatment is conduced before the grating is made by pre-exposing the fiber uniformly to the UV radiation to prevent deformation of the grating index profile. Uniform UV pre-exposure is achieved by translating the stage step by step so that the 244 nm Gaussian-shaped UV beam partially overlaps to write on a large length of the photosensitive fiber, forming a uniform DC index change in advance. The pre-UV flux is estimated to be around 59.5 J/cm^2. The pre-UV flux is applied at the point between the linear region and nonlinear region in Fig. 2b. The middle of the pre-exposed region is then exposed to holographic Gaussian UV beam to write the FBG. Fig. 3a displays the refractive index modulation profiles for specific exposed UV flux following pre-UV treatment. Fig. 3b plots the peak refractive index modulation as a function of the UV exposure flux at the center of the grating following pre-UV treatment. Notably, the index modulation now depends linearly on the UV exposure flux and the induced grating index modulation profiles seem to be Gaussian-like. The $1/e^2$-intensity half widths of the one-shot UV used to generate grating index profile in Fig. 3a were about 6.55 mm, 6.35 mm, and 6.75 mm, similar to the UV beam width of 6.5 mm at a radius of $1/e^2$. This result establishes the linear refractive index response to UV flux after pre-UV treatment. The pre-UV treatment causes the operating point to jump away from the initial nonlinear regime such that the following grating writing process is entirely in the linear regime. The slopes in the linear region of Fig. 2b and in Fig. 3b are 4.15×10^{-7} and 8.22×10^{-7}, respectively, indicating that pre-UV treatment enhanced the photosensitivity. This result is consistent with

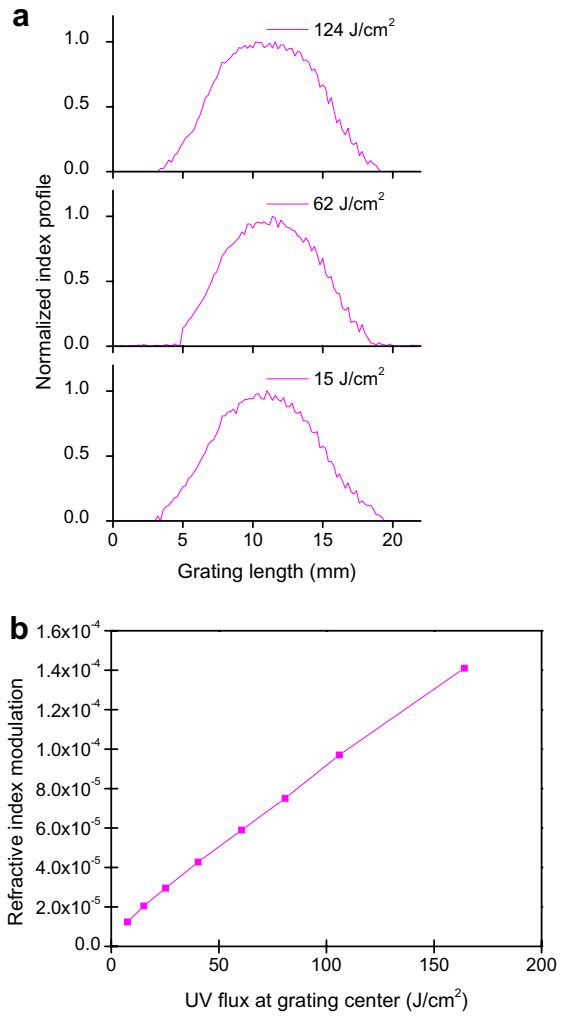

Fig. 3. (a) Refractive index modulation profiles by a single Gaussian UV shot with pre-UV treatment. (b) Refractive index modulation versus UV exposure flux with pre-UV treatment.

the results of previous studies which have demonstrated that photo-hypersensitivity increases the photosensitivity of optical fibers [7]. The pre-UV treatment method is established herein to be a practical method of writing a weak fiber Bragg grating with the target index profile. The narrow-band FBGs were fabricated by using the strongly overlapping step-scan exposure scheme and the real-time interferometric side-diffraction position monitoring method [14] following pre-UV treatment. The side-diffraction interferometric method is developed to connect the sections of gratings precisely. The authors' experience is that obtaining a low noise suppression ratio in the reflection spectrum of under 10 dB without pre-UV treatment is difficult because the nonlinear UV shots overlap process generates imperfections in the apodization index profile.

3. Unequal two-beam interference setup for achieving linear index response

A large grating length and a weak apodized refractive index change with low noise are required to fabricate FBGs with narrow bandwidth and high side-lobe suppression ratio. In the preceding section, pre-UV treatment yields a bias DC UV flux for optical fiber hypersensitization, which is demonstrated to be helpful in ensuring the linear response of the refractive index with AC UV flux. Unfortunately, the two required writing scans are time-consuming and sometimes may generate unwanted uncertainties. This work propose an improved method of interference which uses two unequal beam intensities to provide a bias DC UV flux and to apodize the grating profile at the same time during a single writing scan. Fig. 4a schematically depicts the experimental setup. These two beams, A and B, have different UV fluxes of 24 J/cm^2 and 52.5 J/cm^2, respectively. A half wave plate is placed in one arm of the two linearly polarized beam paths to achieve pure apodization in the sequential UV writing process and thus maintain the same refractive index change along the grating. The whole grating is AC-apodized by setting the two beams with the same polarization at the grating center, and slowly changing the relative polarization of the two beams until these two arms are orthogonally polarized at the grating edge, as in the previous pure apodization setup in which the intensities in the two arms were equal [15]. Fig. 4b plots the variation of the UV flux upon unequal-intensity interference along the fiber axis of the exposed photosensitive optical fiber. When the total UV flux is kept constant along the whole grating, the mean change in the DC index is constant along the grating, achieving true apodization. However, the improved setup turns about 7.5% of the maximum AC UV flux into constant DC bias flux under the same UV exposure conditions, as compared to the true apodization setup in which the intensities of the two arms

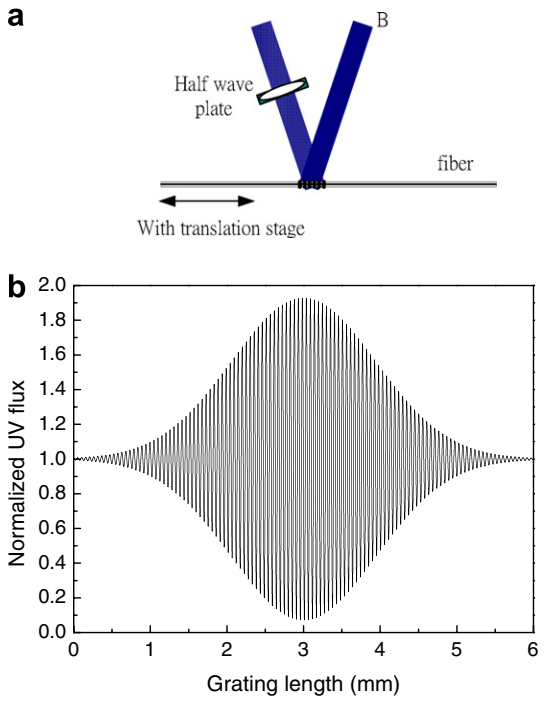

Fig. 4. (a) Experimental setup of unequal two-beam interference. The intensity ratio of beam A and beam B is 0.45. (b). Illustration of UV flux variation versus grating length with unequal-intensity two-beam interference setup.

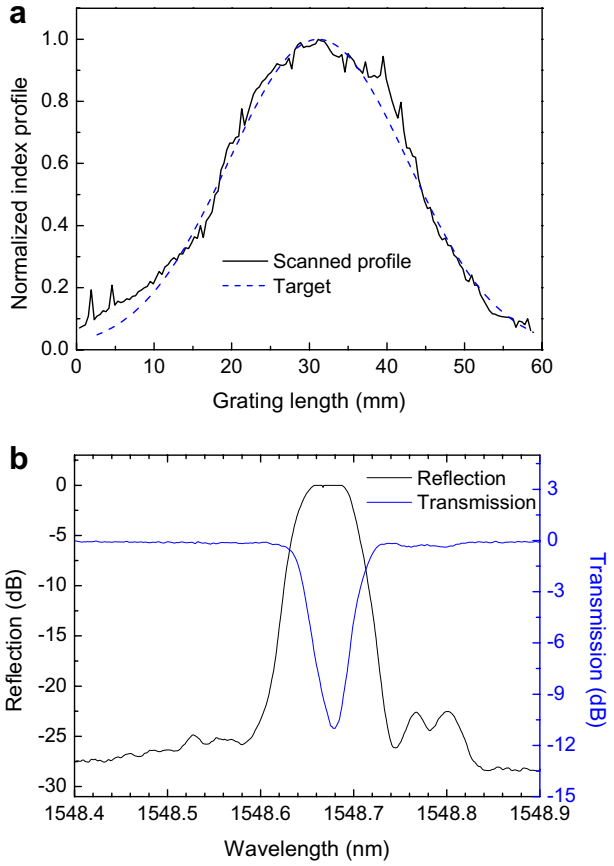

Fig. 5. (a) Refractive index modulation profiles for experimental and target gratings with unequal two beam UV writing. (b) Reflection and transmission spectra of the grating with unequal two beam UV writing.

are equal. Accordingly, the rapidly changing nonlinear index response regime can be avoided from the beginning and the gratings can be inscribed linearly. An experiment is carried out by fabricating a narrow-bandwidth Gaussian apodized FBG with a large length to confirm the feasibility of this proposal. The FBG is connected section by section by several 1.2 mm-spaced UV shots to a total length of 6 cm. Fig. 5a compares the scanned index profile with the target profile. The tail edges are smooth and match the target Gaussian envelope, suggesting the effectiveness of the scheme. Fig. 5b shows the reflection and transmission spectra of the fabricated FBG. The side-lobes are suppressed below 20 dB and the 3 dB bandwidth is approximately 0.05 nm. The peak refractive index change is 3.3×10^{-5}, as determined by simulation fitting. Compared with the equal-intensity interference setup for a given total UV flux, this improved setup is effective in writing FBGs to match the designed index profile. The two beam intensity ratio can be further adjusted to optimize the performance.

4. Conclusion

In conclusion, the nonlinear relationship between the exposed UV flux and the induced index change of the FBGs was calibrated more carefully than before using the side-diffraction method to determine the grating profile. The pre-UV treatment method was demonstrated to eliminate the nonlinear index-change response regime when the UV flux is low. An alternative new method of unequal two-beam interference was demonstrated to be able to ensure further that the shape of the induced index profile matched the targeted apodized envelope. The authors assert that the methods and the results presented in this work will be very useful in fabricating long narrow-band FBGs with weak refractive index profiles.

Acknowledgements

This research is partially supported by the National Science Council of the Republic of China under the contract NSC 95-2221-E-009-223 and NSC 95-2752-E-009-009-PAE.

References

[1] Xiaoxu Li, Cheolhwan Kim, Guifang Li, Opt. Express 12 (2004) 3196.
[2] T. Qiu, S. Suzuki, A. Schülzgen, L. Li, A. Polynkin, V. Temyanko, J.V. Moloney, N. Peyghambarian, Opt. Lett. 30 (2005) 2748.
[3] L.-G. Sheu, K.-P. Chuang, Y. Lai, IEEE Photon. Technol. Lett. 15 (2003) 939.
[4] K. Kolossovski, R. Sammut, A. Buryak, D. Stepanov, Opt. Express 11 (2003) 1029.
[5] C.-L. Lee, R.-K. Lee, Y.-M. Kao, Opt. Express 14 (2006) 11002.
[6] H. Patrick, S.L. Gilbert, Opt. Lett. 18 (1993) 1484.
[7] A. Canagasabey, J. Canning, N. Groothoff, Opt. Lett. 28 (2003) 1108.
[8] P.A. Krug, R. Stolte, R. Ulrich, Opt. Lett. 20 (1995) 1767.
[9] J. Canning, M. Janos, M.G. Sceats, in: 20th Australian Conference on Optical Fibre Technology (ACOFT-20), Coolum, Queensland, December, 1995, p. 303.
[10] J. Canning, M. Janos, M.G. Sceats, Opt. Lett. 21 (1996) 609.
[11] L.M. Baskin, M. Sumetsky, P.S. Westbrook, P.I. Reyes, B.J. Eggleton, IEEE Photon. Technol. Lett. 15 (2003) 449.
[12] F. El-Diasty, A. Heaney, T. Erdogan, Appl. Opt. 40 (2001) 890.
[13] John Canning, Opt. Fiber Technol. 6 (2000) 275.
[14] K.-C. Hsu, L.-G. Sheu, K.-P. Chuang, S.-H. Chang, Y. Lai, Opt. Express 13 (2005) 3795.
[15] K.-P. Chuang, Y. Lai, L.-G. Sheu, IEEE Photon. Technol. Lett. 16 (2004) 834.